MACROSCOPIC EROSION OF DIVERTOR MATERIALS UNDER PLASMA HEAT LOADS TYPICAL FOR ITER HARD DISRUPTIONS.

V.Safronov[1], N.Arkhipov[1], V.Bakhtin[1], V.Barsuk[1], S.Kurkin[1], E.Mironova[1], G.Piazza[2], H.Würz[2], A.Zhitlukhin[1]

[1] Troitsk Institute for Innovation and Fusion Research, 142190 Troitsk, Moscow reg., Russia
[2] Forschungszentrum Karlsruhe, P.O. Box 3640, 76021 Karlsruhe Germany

PACS: 52.40.Hf; 52.55.Rk

1. INTRODUCTION

During tokamak plasma disruptions, the divertor components in ITER will be exposed to an intense flow of hot plasma. Disruption heat fluxes will cause erosion of plasma facing materials. Erosion restricts a lifetime of the divertor components and produces a substantial amount of the material dust, which being tritiated, radioactive and chemically reactive presents a serious problem for a safety. The exact amount and properties of eroded material is critically important to lifetime and safety analysis of tokamak-reactor.

The divertor heat loads in ITER are estimated to be 1-10 kJ/cm^2 for the thermal quench phase (1–10 ms) of disruptions [1]. Since the expected heat loads are not achievable in existing tokamaks, plasma-induced erosion is investigated by using powerful plasma devices [2-6] capable to simulate, at least in part, the loading conditions of interest. The results of the disruption simulation experiments are used for development and validation of appropriate numerical models [7,8].

Experimental and theoretical investigations [9,10] have shown that disruptive heat load results in a sudden evaporation of a thin surface layer of the irradiated material and produces a cloud of dense vapor plasma. The vapor plasma acts as a thermal shield: it stops the plasma stream and protects the surface from the direct action of the hot plasma. The target plasma dissipates the incoming energy flux into photon radiation thereby reducing the surface heat load. Due to the vapor shielding effect, the material vaporization decreases considerably.

The available data permit to determine the heat flux reaching the surface under tokamak disruption and thus to estimate a mass of evaporated material. However, plasma-induced erosion results not solely from the vaporization but also from macroscopic erosion processes such as brittle destruction for carbon-based materials [6,11] and melt layer splashing for metals [12]. The erosion products are emitted as droplets (metals) and grains (CBMs). Investigation of macroscopic erosion is of great importance because at adequate heat loads the macroscopic processes might lead to greater surface damages and greater amount of dust than vaporization.

In the present work, graphite, carbon-fibre composites and a set of metallic targets have been tested in disruption simulation experiments at the MK-200UG facility [3]. Erosion mechanisms and their contribution to the net material erosion were investigated. Properties of erosion products were studied as well.

2. EXPERIMENTAL

The basic scheme of the MK-200UG facility is shown in Fig.1. The facility consists of a pulsed plasma gun, a long drift tube and a target chamber.

The plasma gun is fed from 1152μF capacitor bank at operating voltage of 25kV. It corresponds 360kJ energy stored in the capacitor bank.

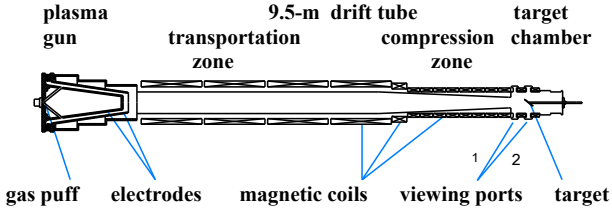

Fig.1. Basic scheme of the MK-200UG facility.

The plasma gun injects a hydrogen plasma stream into the drift tube, consisting of 6.5-m cylindrical part and of a conical one with a length of 3m. Diameter of the cylindrical tube is 30cm. At the conical section, the tube diameter reduces towards its exit from 30cm to 15cm. The cylindrical tube is filled with a 0.7T longitudinal magnetic field. The magnetic field rises from 0.7T up to 2.5T along the conical part.

Samples are placed at the end of the drift tube in the target chamber equipped with diagnostic tools. Magnetic field is 2T in the target chamber. Parameters of hydrogen plasma stream at the target position are shown in Table1.

Table 1. Plasma stream parameters at the MK-200UG.

energy density	q = 1.5 kJ/cm^2
pulse duration	τ = 40 - 50 μs
impact pressure	P = 8 – 10 atm
directed ion energy	E_i = 1.5 keV
plasma density	n = (2 - 6)×10^{15} cm^{-3}
electron temperature	T_e = 100 – 200 eV
beta value, 8πP/B^2	β = 0.3
diameter	D = 6 – 7 cm

Total energy of the plasma stream is about 50 kJ.

The targets were manufactured as rectangular plates with the dimensions larger than the plasma stream diameter. Thus the targets overlapped fully the plasma stream.

Erosion crater was analysed by use of the mechanical profilometer. The mass loss was measured by weighting the target before and after the plasma irradiation. Surface

damage was investigated by means of optical microscope and scanning electron microscope (SEM).

Erosion products (carbon particles and metal droplets) were collected at the special collectors placed around the target. The collected erosion products were analysed using an optical microscope provided with a CCD camera, and the size of the particles and droplets was measured. Erosion products of carbon-based materials were studied also by X-ray diffractometry in order to determine a percentage of crystalline graphite particles in the erosion products.

Laser scattering technique was applied for on-line measurement of the emitted particles and droplets.

3. EXPERIMENTAL RESULTS

3.1. Carbon-based materials (CBMs)

Graphites and carbon fiber composites consist of graphite granules. Pulsed heat load produces a thermal stress in the exposed sample. When the thermal stress value at the inter-granular bond exceeds the bond failure stress then the bond breaks [13]. Therefore, brittle destruction occurs and graphite dust is produced.

3.1.1. Graphite

Table 2 shows the erosion of MPG-8 graphite. Perpendicular (90°) and tilted at the angle 60°, 40°, and 20° targets were examined.

Table 2. Erosion of MPG-8 graphite.

angle	90°	60°	40°	20°
erosion (μm/shot)	0.4	0.4	0.34	0.22

Maximum erosion was measured to be 0.4 μm/shot at perpendicular plasma impact. Energy, which is required for vaporization of such graphite layer, is of 3 J/cm^2 that corresponds to 0.2% of the plasma stream energy (Q=1.5 kJ/cm^2). Quite small erosion is explained by the shielding effect. With no shielding effect, when the plasma stream energy Q is consumed completely for graphite heating and vaporization, the erosion rate would be about 200 μm/shot [9].

The erosion products are emitted in a form of carbon vapor and carbon particles. The carbon vapor deposits at nearby components and produces redeposited carbon layers. Redeposited carbon has an amorphous structure [14]. The particles maintain the original phase structure of MPG-8 graphite having a hexagonal crystal structure.

The erosion products collected near the exposed graphite target were analyzed by X-ray diffractometry. About 5–10 % of the collected erosion products were crystalline particles. As the particles are formed due to brittle destruction, one could conclude that brittle destruction contributes only a little (5–10 %) to the net erosion. However, the real contribution of macroscopic erosion might be considerably greater because the eroded particles are evaporated in the plasma shield near the target surface. As shown in [14] all the particles with a size smaller than 6 μm will be completely vaporized if they are formed at the beginning of plasma exposure. Therefore only the particles formed later and the particles of greater size can be detected in the collected erosion products. The question on the contribution of brittle destruction to the net erosion remains open.

Fig.2 shows the size distribution of the carbon particles. The distribution is peaked at 1-3 μm. Almost 80% of the collected particles are in this range. Large particles are present also but their percentage reduces quickly with the particle size. The measured size of particles agrees well with the size of the granules observed by SEM at the exposed graphite surface (Fig.3).

Because of their small size a large fraction of the emitted particles are vaporized near the target that results in additional surface shielding. Therefore, brittle destruction of graphite does not lead to a substantial increase of the net erosion [13].

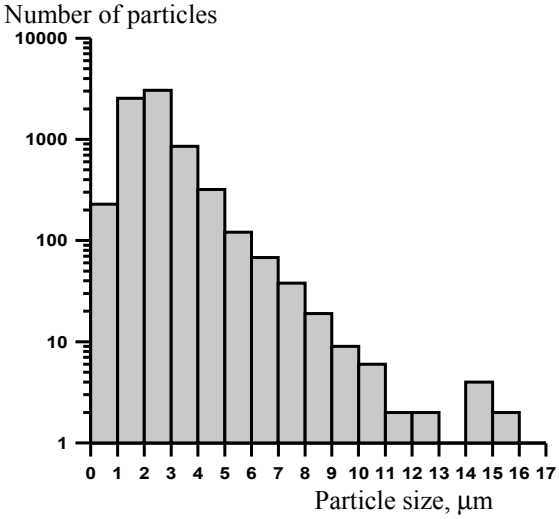

Fig.2. Size distribution of MPG-8 graphite particles.

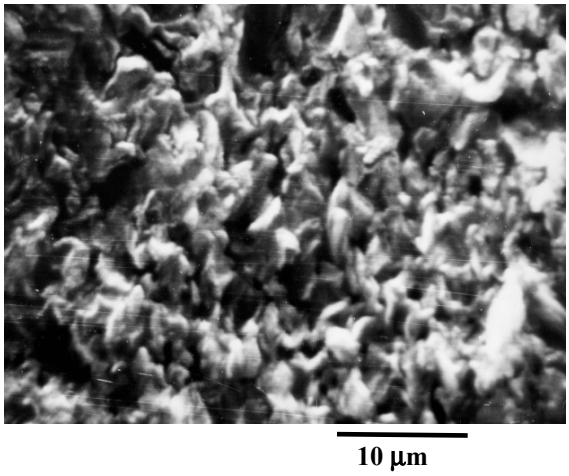

Fig.3. SEM image of exposed graphite surface.

3.1.2. Carbon fiber composites

Carbon fiber composites Sep.Carb. NB31 and NS31 have been tested. They were exposed to 100 plasma shots. The amount of the eroded material was quantified by weighting the CFC samples before and after plasma exposure. The mass loss was measured after each set of 10 shots, then the magnitude of Δm was evaluated for one shot. The mass loss of graphite was also studied. There was measured that the magnitude of Δm increases slowly in CFC with a number of plasma shots and after 70-80 shots it becomes practically the same as in graphite.

Plasma-induced damages of CFC differ from the graphite damages. Plasma irradiation results in formation of cracks and open holes at the CFC surface (Fig.4). Typical size of the hole is 100-200 microns. After 100 plasma exposures, the holes cover about 10% of the CFC face surface. The holes arise because of brittle CFC destruction and emission of the debris. Among the erosion products there are debris of 50-150 microns. Formation

of cracks and holes might cause a degradation of the CFC properties and an increase of the net erosion in the following plasma shots.

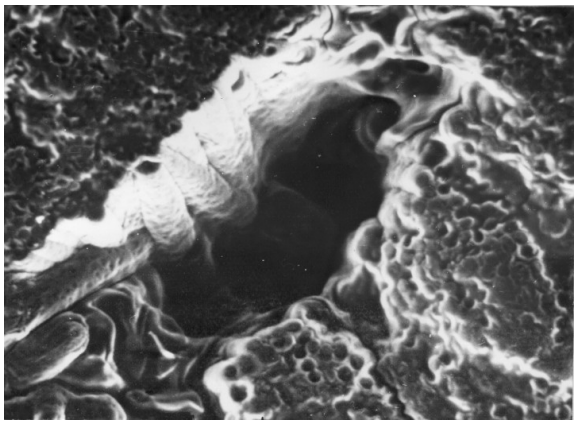

Fig.4. SEM image of exposed NS31 surface.

3.2. Metals

Interaction of intense plasma streams with metal targets results in the formation of a melt layer. The liquid metal is subjected to different forces, which can lead to the melt splashing (Fig.5) and macroscopic erosion. The melt boiling and hydrodynamic instabilities in the liquid metal results in emission of the droplets.

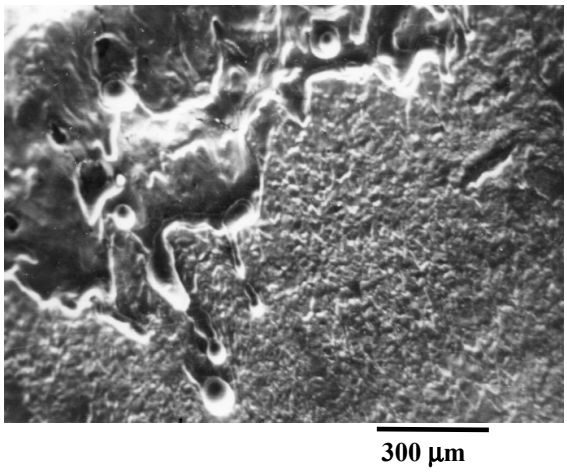

Fig.5. Tungsten melt splashing.

The melt layer erosion have been studied in the experiments with aluminum, copper, titanium and tungsten. There was found that the main mechanism of the melt layer erosion is the melt movement. Under the plasma stream action, the melt moves in radial direction along the exposed surface from the stream axis to periphery. The melt movement results in a formation of the erosion crater and the melt mountains at the crater edge. The erosion crater and mountains grow linearly with a number of shots. The measured erosion rate for copper is about 4 μm/shot. The mountains grow with a rate 7-8 μm/shot. The net volume of the mountains is equal to the net volume of the erosion crater i.e. there is a balance of the material eroded and the material accumulated in the mountains. The exposed surface demonstrates a large roughness (up to 100 μm) because of melt boiling and formation of the surface waves.

The melt layer injects droplets. The droplet size varies from a few microns to a few tens microns. The velocity of the droplets depends on their size: the smaller size - the greater velocity. The velocity of micron droplets is 1-10 m/s. Droplet injection contributes only a little to the net erosion. The erosion rate evaluated from the measured mass loss is 0.1-0.15 μm/shot for all the metal targets.

Macroscopic erosion of tungsten results not solely from the melt splashing but also from the surface cracking (Fig.6). Under the thermal cycling test [15] followed the disruption test the cracks propagate into the sample body and volumetric cracking occurs. A majority of the tungsten grades is damaged due to volumetric cracking. W-5Re-0.1ZrC alloy shows the best performance.

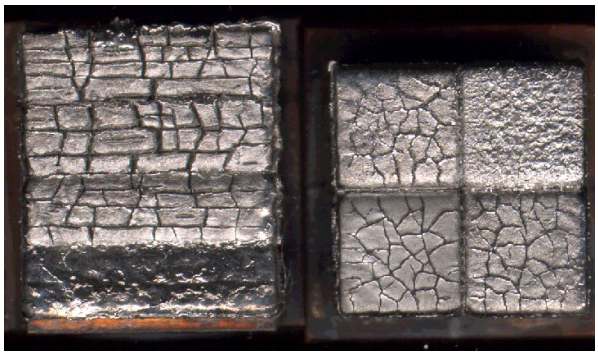

Fig.6. Tungsten cracking.

4. SUMMARY

Macroscopic erosion of carbon-based materials and metals has been studied in disruption simulation experiments at the MK-200 plasma gun facility.

Macroscopic erosion of carbon based materials results from brittle destruction. In graphite, the erosion products are emitted as micron particles. The small particles are vaporized near the target that leads to additional surface shielding and a reduction of the resultant erosion.

In carbon-fibre composites, the surface cracks and the open holes (100-200 μm) are formed due to brittle destruction. The erosion might increase with a number of exposures because of degradation of the CFC properties.

Melt layer movement along the exposed surface is a general erosion mechanism for metallic targets. Evaporation and emission of droplets contribute only a little (< 10%) to the net erosion. Surface damages in tungsten are caused mainly by cracking.

The present knowledge on macroscopic erosion is insufficient to extrapolate the available data to ITER disruption conditions.

5. REFERENCES

1. G.Federici et al., Nucl. Fusion. 41 (2001) 1967.
2. V.Kozhevin et al., Fusion Eng. Des. 28, (1993), 157.
3. N.Arkhipov et al., J.Nucl. Mater. 233-237, (1996), 767.
4. V.Belan et al., J.Nucl. Mater. 241-243, (1996), 763.
5. V.Chebotarev et al., J.Nucl. Mater. 233-237, (1996), 736.
6. V.Astrelin et al., Nucl. Fusion 37 (1997) 1541.
7. H.Würz et al., Fus. Science and Technol. 40 (2001) 191.
8. A.Hassanein et al., Plasma Devices and Operations, 5, (1998) 297.
9. H.Würz et al., Fusion Technology, 32, (1997), 45.
10. V.Safronov et al., J.Nucl. Mater. 290-293 (2001) 1052.
11. M.Guseva et al., J.Nucl. Mater. 220-222 (1995) 957.
12. V.Litunovsky et al., Proc. of 20th SOFT, Marseille, France, 7-11 September, 1998. V.1. P.59.

13. S. Pestchanyi et al., Physica Scripta T91 (2001) 84.
14. F. Scaffidi-Argentina et al., J.Nucl. Mater. 283-287 (2000), 1111.
15. A. Makhankov et al., Proc. of 20th SOFT, Marseille, France, 7-11 September, 1998. V.1, 267.